ELSEVIER

International Journal of Pharmaceutics 243 (2002) 93–105

international journal of pharmaceutics

www.elsevier.com/locate/ijpharm

Preparation, characterization and biodistribution of ultrafine chitosan nanoparticles

Tanima Banerjee [a], Susmita Mitra [a], Ajay Kumar Singh [b], Rakesh Kumar Sharma [b], Amarnath Maitra [a,*]

[a] *Department of Chemistry, University of Delhi, Delhi 110007, India*
[b] *Institute of Nuclear Medicine and Allied Sciences, Brig S.K. Mazumdar Road, Delhi 110054, India*

Received 15 November 2001; received in revised form 3 May 2002; accepted 8 May 2002

Abstract

Chitosan nanoparticles cross-linked with glutaraldehyde have been prepared in AOT/*n* hexane reverse micellar system. The cross-linking in the polymeric network has been confirmed from FTIR data. Because of the adhesive nature of these particles, their sizes, as measured by QELS, have been found dependent on the particle density in aqueous buffer. The particle size has also been found to vary with the amount of cross-linking. The actual particle size of these chitosan nanoparticles with a particular degree of cross-linking has been determined at infinite dilution of particles in water. The particle size at infinite dilution is ≈ 30 nm diameter, when 10% of the amine groups in the polymeric chains have been cross-linked and it shoots up to 110 nm diameter when all the amine groups are cross-linked (100% cross-linked). TEM pictures show that these particles are spherical in shape and remain in the form of aggregation. The biodistribution of these particles after intravenous injections in mice showed that these particles readily evade the RES system and remain in the blood for a considerable amount of time. The γ image of the rabbit after administration of ^{99m}Technetium (^{99m}Tc) tagged chitosan nanoparticles also confirms the above observation, as the blood pool is readily visible even after 2 h. The γ picture shows distribution of particles in the heart, liver, kidneys, bladder and the vertebral column. Interestingly, the biodistribution studies of the chitosan nanoparticles have indicated that these particles are distributed in the bone marrow also, implying the possibility of using these nanoparticles for bone imaging and targeting purpose. © 2002 Published by Elsevier Science B.V.

Keywords: Chitosan nanoparticles; Gamma imaging; Biodistribution; Hydrogel polymers; ^{99m}Technetium

1. Introduction

Chitosan is an interesting natural material occurring in abundance in the environment. Its excellent biocompatibility and several advantages due to its unique polymer cationic character renders it highly useful for pharmaceutical application (Thanoo et al., 1992; Illum, 1998). A polysaccharide comparable to cellulose, comprising copolymers of glucosamine and *N*-acetyl glucosamine linked by β-(1–4) linkages, chitosan can be derived by partial deacetylation of chitin from crustacean shells. The primary amino groups lead

* Corresponding author. Tel.: +91-11-7666-593
E-mail address: maitra@giasdl01.vsnl.net.in (A. Maitra).

0378-5173/02/$ - see front matter © 2002 Published by Elsevier Science B.V.
PII: S0378-5173(02)00267-3

to special properties that render chitosan very interesting for pharmaceutical applications (Kristl et al., 1993). In contrast to most other natural polymers, it has a positive charge and is mucoadhesive (Berscht et al., 1994).

Besides other applications (Felt et al., 1998), chitosan has been extensively examined for its potential in the development of controlled release drug delivery systems (Kawashima et al., 1985; Thanoo et al., 1992; Akbuga, 1993) and these controlled release formulations have been made in the form of chitosan gels (Kristl et al., 1993), tablets (Nigalaye et al., 1990) and capsules (Tozaki et al., 1997), in addition to microspheres and microcapsules (Nishioka et al., 1990; Aiedeh et al., 1997). Nanoparticles have a special role in targeted drug delivery in the sense that they have all the advantages of liposomes including the particle size, but unlike liposomes, nanoparticles have a long shelf life and can usually entrap more drugs than liposomes. Although nanoparticles made of hydrophobic polymers encapsulating hydrophobic drugs have been reported in the literature, very few studies have been made on the preparation of drug-loaded hydrogel nanoparticles (Mitra et al., 2002). Nanoparticles made of hydrophobic polymers are usually taken up by RES and have short residence time in blood (Douglas et al., 1986). The surfaces of these hydrophobic nanoparticles are made hydrophilic by conjugating with the polyethylene glycol (PEG) type of molecules to make these particles long circulating in blood. We have recently optimized a method of preparation of ultra low size nanoparticles of hydrogel polymers and have been able to load water-soluble drugs into them (Maitra et al., 1999). These hydrophilic nanoparticles evade RES and remain in circulation for a couple of hours without PEG conjugation on the particle surface. These hydrogel polymers can have reactive groups on the surface which enable the nanoparticles to be converted to stimuli responsive particles and they can also be made targetable by attaching receptor specific ligands. The preparation of nanoparticles from chitosan, a hydrogel polymer, for drug delivery can have several advantages over the use of chitosan microspheres and microcapsules. Nanometer range particles have easy accessibility in the body, being transported via the circulation to different body sites. Extremely small nanoparticles, of < 100 nm diameter with hydrophilic surface, have been found to have longer circulation in blood (Allemann et al., 1993). Such systems should allow the control of the rate of drug administration that prolongs the duration of the therapeutic effect, as well as the targeting of the drug to specific sites.

Preparation of nanoparticles with this versatile hydrogel material has been attempted by several workers with the purpose of utilizing its mucoadhesive properties to transport drugs and DNA across mucosal surfaces (Alonso et al., 1998; Roy et al., 1999). The polycationic nature of deacetylated chitosan results in polycondensation in the presence of anionic macromolecules. Thus, chitosan–DNA nanoparticles can be prepared by the method of coacervation (Roy et al., 1999). Besides, the reactive free amino group on the particle surface makes it possible to chemically conjugate various other reactive groups, such as polyethylene glycol (PEG) derivatives, different ligands, antibodies and other pH and temperature sensitive moieties (MacLaughlin et al., 1998). Several methodologies have also incorporated other polymers in the preparative procedure, with the intent of preparing smart hydrophilic nanoparticles under extremely mild conditions (Calvo et al., 1997).

Considering the advantages of using ultra low sized hydrophilic nanoparticles for drug delivery, we have focussed on the preparation of chitosan nanoparticles of < 100 nm diameter. Preparation of nanoparticles using reverse micelles as a medium makes it possible to produce ultrafine particles with narrow size distribution (Leong and Candau, 1982; Munshi et al., 1995). The aqueous core of the reverse micellar droplets can be used as nanoreactor to prepare these particles, since the size of the reverse micellar droplets is in the nanometer range and these droplets are highly monodispersed (Maitra, 1984). The present paper describes the preparation of cross-linked chitosan nanoparticles of size < 100 nm diameter using reverse micelles as the media and their physicochemical characterization as well as biodistribution.

2. Experimental

2.1. Materials

Chitosan (M.W. 400 kDa), glutaraldehyde, surfactant i.e. sodium bis(ethylhexyl) sulfosuccinate (AOT), were purchased from Sigma (St. Louis, MO). All other reagents used were of analytical grade. Sodium pertechnetate separated from Molybdenum -99 by solvent extraction method was procured from the Regional Center for Radiopharmaceutical (Northern Region), Board of Radiation and Isotope Technology, Delhi, India.

2.2. Preparation of cross-linked chitosan nanoparticles

Chitosan nanoparticles were prepared by modifying the reverse micelle medium using a method previously reported by us (Maitra et al., 1999). A brief outline of the method is as follows. The surfactant, AOT, was dissolved in *n*-hexane (0.04–0.1 M solution). To 40 ml of (0.04 M) AOT solution, 400 μl of 0.1% w/v chitosan solution in 6% v/v acetic acid, 176 μl of Tris–HCl buffer (0.01%; pH 8.0), 40 μl liquor ammonia, 4 μl of 0.01% v/v glutaraldehyde solution were added, with continuous stirring at room temperature. The solution was homogenous and optically transparent. The system was left, under stirring, overnight at room temperature. The above method produced placebo chitosan nanoparticles with 10% cross-linkage. The solvent was then evaporated off in a rotary evaporator and the dry mass resuspended in 20 ml of Tris–HCl buffer (pH 8.0) by sonication. Some 4 ml of 30% $CaCl_2$ solution was added dropwise to precipitate the surfactant as calcium salt of diethylhexylsulphosuccinate ($Ca(DEHSS)_2$). The precipitate was pelleted by centrifugation at 6000 rpm for 15 min at 4 °C. The cake of $Ca(DEHSS)_2$ after centrifugation contained some adsorbed nanoparticles. It was dissolved in 10 ml *n*-hexane and the hexane solution washed two to three times, each time with 1 ml of Tris–HCl buffer. The phase-separated aqueous layer was drained out and added to the original centrifugate. The total aqueous dispersion of nanoparticles was then dialyzed for ≈ 2–3 h using a Spectrapore membrane dialysis bag (12 kDa cut off). The dialyzed solution was lyophilized to dry powder for subsequent use. Lyophilized nanoparticles are easily redispersable in aqueous buffer. To produce nanoparticles with a different degree of cross-linking, a calculated amount of glutaraldehyde is added such that the desired percent of free amine groups of chitosan conjugate with glutaraldehyde, assuming 100% conjugation efficiency. The flow diagram for the preparation of chitosan nanoparticles in reverse micelles is shown in Fig. 1.

2.3. Size and morphology of the nanoparticles

Quasi-elastic light scattering (QELS) measurements and transmission electron microscopy (TEM) were used to establish the size and morphology of the chitosan nanoparticles.

2.3.1. Quasi-elastic light scattering (QELS)

QELS was performed using Brookhaven 8000 (USA) instrument with BI200SM Goniometer, air-cooled argon ion laser operated at 488 nm as the light source using 128-channel digital correlator. The time dependence of the intensity autocorrelation function of the scattered intensity was derived which gave the self-diffusion of the particles. The size of the nanoparticles was determined from the diffusion of the particles (D) using Stoke–Einstein equation

$$d_h = \frac{kT}{3\pi\eta D}$$

where k is the Boltzmann constant, T is the absolute temperature, η is the viscosity of the medium and d_h is the hydrodynamic diameter of the particles. Lyophilized powder (100 μg) was dispersed in 2 ml water by vortexing and used for QELS measurement. The sample was subsequently diluted to give nanoparticle solutions of known concentration and the particle size distribution was measured. Nanoparticle with different degree of cross-linking, were similarly diluted for measurement of size distribution.

2.3.2. Transmission electron microscopy (TEM)

Lyophilized powder (100 μg) was dispersed in 5 ml distilled water to have a clear solution. Samples for TEM were prepared using the above clear solution. The sample solution was put on a formvar coated grid (1% solution of formvar was prepared in spectroscopic grade chloroform). A clean glass slide was dipped in formvar solution to make a formvar film on the stars, the glass slide was scratched on the edges and the forvmar film were floated on distilled water on a spherical container, the 2090 mesh copper grids were placed upside down on the floating plastic film. A piece of water filter paper was blotted on the plastic film and lifted out from the distilled water. In this way, the plastic coated grids were prepared. On this grid, a drop of the sample solution (containing dispersed nanoparticles) was placed and allowed to air-dry. A TEM picture was taken in a JOEL JEM 2000 EX200 microscope.

2.3.3. FT-IR studies

The IR spectra of chitosan nanoparticles were taken in KBr pellet using Perkin-Elmer Fourier transformed infrared (FT-IR) spectrophotometer (spectrum 2000) instrument.

2.4. Radiolabeling of placebo chitosan nanoparticles

Lyophilized chitosan nanoparticles (1 mg/ml) were dispersed in Tris–HCl buffer (pH 7.2) Nitrogen purging, prior to mixing was carried out to degas all solutions. To 200 μg ^{99m}Tc (2.2 mCi) in saline, 5 mg of solid sodium borohydride was added directly with continuous stirring followed by immediate addition of 400 μg of the above chitosan nanoparticles dispersed in buffer. The solution was stirred for 20 min at room temperature The contents were filtered using 0.22-micron filter (Millipore Corporation) into an evacuated sterile sealed vial and quality control was per-

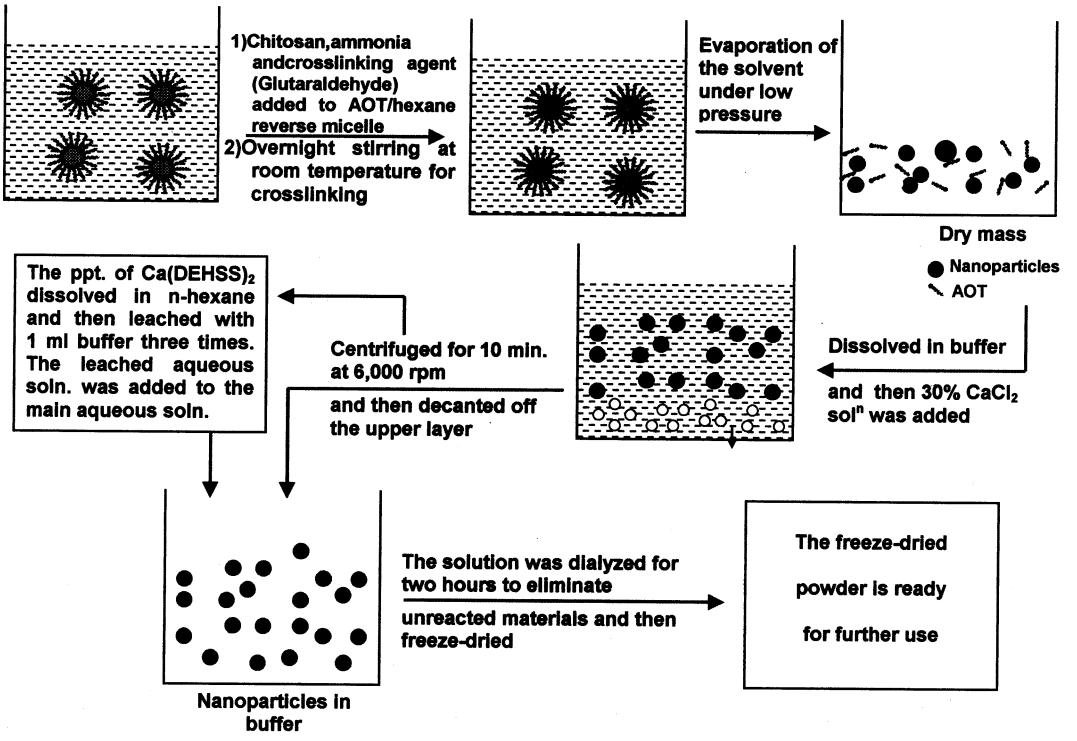

Fig. 1. Flowchart of preparation of cross-linked chitosan nanoparticles.

formed following the method described earlier (Theobald, 1990).

The labeling efficiency of ^{99m}Tc to chitosan nanoparticle was assessed by ascending instant thin layer chromatography (ITLC) using silica gel coated fiber sheets (Gelman Sciences Inc., Ann Arbor, MI). The ITLC was performed using acetone as the mobile phase. The free pertechnetate which moved with the solvent ($R_f = 0.9$) was estimated as 15–20% of the total radioactivity added. Labeling efficiency was calculated using the following equation

$$\text{Labeling efficiency } \% = \frac{\text{Total counts} - \text{counts of free pertechnetate}}{\text{Total counts}} \times 100$$

2.5. Stability study of ^{99m}Tc-chitosan nanoparticles complex

The stability study of the radiolabeled chitosan nanoparticles was determined in vitro by ascending ITLC. A total of 400 μg of labeled chitosan particles (1 mg/ml) in Tris–HCl buffer (pH 7.2) was incubated at 37 °C. ITLC was performed at different time intervals to assess the stability of the complex.

2.6. Biodistribution studies

Biodistribution of ^{99m}Tc-chitosan nanoparticles was studied in 2–3 month-old Swiss albino mice. An injected dose of 100 μl (1 mg/ml) of sterile radiolabeled nanoparticle suspension was administered through the tail vein of each mice, weighing 25–30 g. The animals were sacrificed by cervical dislocation at different time intervals and different organs were removed, washed with normal saline and dried in paper folds. The radioactivity in each organ was counted using well-type γ spectrometer and expressed as percent injected dose per organ, taking into account the physical decay in a standard sample.

2.7. Statistical analysis

Data have been represented as the mean of six individual observations with S.E.M. Significance has been calculated using Student's t-test.

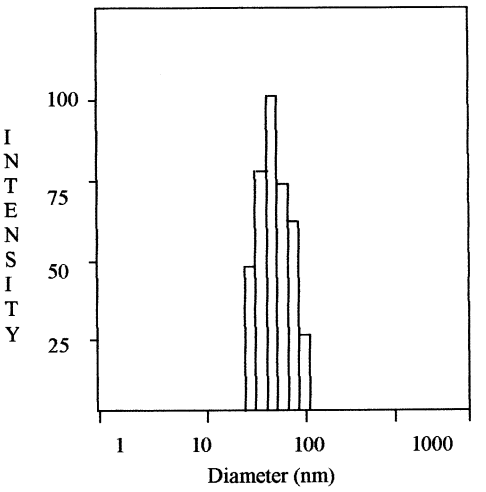

Fig. 2. Size distribution of chitosan nanoparticles by QELS.

2.8. Gamma-imaging

For γ-imaging studies, New Zealand rabbit (weight 2.0–2.5 kg) was used. After intravenous administration of 1 ml of radiolabeled nanoparticles (400 μg/ml) through the dorsal vein of the ear, the animal was anesthetized by intramuscular injection of 1 ml ketamine hydrochloride and 1 ml calmpose. The animal was fixed on a board in posterior anterior position and imaging was performed at different time intervals using a planar γ camera.

3. Results and discussion

3.1. Characterization of chitosan nanoparticles

3.1.1. Size of the nanoparticles

We have determined the particle size by quasi-elastic light scattering measurements. A representative spectrum is shown in Fig. 2. Chitosan is an adhesive hydrogel polymer (Robert et al., 1988). Therefore, in aqueous solution, these nanoparticles interact among themselves through their Brownian motion to form clusters. For interacting particles, the average particle size is always found higher than the actual size of the particles. The diffusion

coefficient, D, of these interacting particles can be studied by QELS. In the low concentration range, D can be written as (Hou et al., 1988)

$$D = D_o(1 + \alpha\phi)$$

where D_o is the intrinsic diffusion coefficient at infinite dilution when the interaction among the particles is zero and α is the virial coefficient of diffusion and is dependent on the interacting potential among the particles, ϕ is the volume fraction of the particles in the medium. The hydrodynamic diameter, d_h, of the dispersed particles is related to the particle diffusion (D) through Stokes–Einstein equation as mentioned earlier. Self-adhesive polymers tend to produce particle aggregation leading to the formation of large particles due to strong interparticle interaction (Bernkop-Schnurch and Krajicek, 1998). With progressive dilution, the inter-particle interaction is reduced and at infinite dilution, when the inter-particle interaction is practically zero, the particle size (projected) becomes exactly same as the actual size of the particles (d_h^o). As shown in Fig. 3, we have measured the sizes of the dispersed particles from their apparent diffusion coefficient at various particle densities for particles with different degree of cross-linking. The figure in the inset shows the variation of particle size d_h^o; at infinite dilution, with degree of cross-linking. The particle size increases exponentially with the increase of degree of cross-linking. In addition to the clustering due to the self-adhesiveness of the polymeric materials in the nanoparticles, the probability of interparticle cross-linking through glutaraldehyde is also increased with the increased concentration of cross-linking agent (Munshi, et al., 1997).

From the inset in Fig. 3 it can be clearly observed that an increase in percentage cross-linking from 10 to 100% results in an increase of particle size from 30 to $\approx$110 nm diameter at infinite dilution. Thus, at an intermediate dilution, when the particle size is $\approx$75 nm diameter for a 10% cross-linked polymer, it is 500–600 nm diameter for 100% cross-linked polymer at the same dilution. Observations of TEM reveal more or less spherical morphology of the nanoparticles. Nanoparticles of lower cross-linking (10%) appear as smaller aggregates having size range < 50 nm (Fig. 4a), while at higher cross-linking (100%), much larger particles are observed, which appear as highly dense aggregates (Fig. 4b).

3.1.2. FTIR-studies of cross-linked chitosan nanoparticles

The chitosan nanoparticles were prepared by cross-linking the polymer with glutaraldehyde within the reverse micelles. Fig. 5(a,b) exhibit the FTIR spectra of chitosan and chitosan nanoparticles, respectively.

As seen in Fig. 5(a), the strong peaks in the range 3400–3200 cm^{-1} correspond to combined peaks of hydroxyl and intramolecular hydrogen bonding. Primary amines also show sharp absorption at 3500 and 3400 cm^{-1} arising from the asymmetric and symmetric stretching of 2 N–H bonds, but the peaks appear broad here due to the contributed peaks of O–H stretching and hydrogen bonds. For crosslinked chitosan nanoparticles, an additional peak at 1634 cm^{-1} can be observed in Fig. 5(b), which corresponds to stretching vibrations of C = N bond. This strong peak indicates the formation of Schiff's base as a result of the reaction between carbonyl group of glutaraldehyde and amine group of chitosan chains. However, this peak is associated with another peak corresponding to the NH_2 scissoring vibration seen at 1650 cm^{-1} of the primary amines in chitosan chains, which can be easily detected when one compares the spectra of the simple chitosan and cross-linked chitosan polymer, as shown in Fig. 5(a,b). The C–H stretching vibration of the polymer backbone is manifested through strong peak at 2926 cm^{-1}. Acetyl groups absorb in the range 1300–1100 cm^{-1}, as seen in Fig. 5. The peaks in the fingerprint region of the spectrum are given by ethereal bonds, where the symmetric stretch of C–O–C is found around 1020–1075 cm^{-1}.

3.2. Radiolabeling efficiency of chitosan nanoparticles

About 80–85% of ^{99m}Tc was found to form complex with the nanoparticles, as calculated

from the radiolabeling efficiency equation. The rest of the ^{99m}Tc ions remain as free pertechnetate ions ($\approx$15–20%). Labeled-chitosan nanoparticle complex (400 μg) was found stable up to 80–85% in the first 2 h, as calculated from the above equation. The free pertechnetate, which was 15–20% up to 4 h, increased to $\approx$70% after 24 h of incubation.

3.3. Biodistribution of nanoparticles

The biodistribution of radiolabeled chitosan nanoparticles after 30, 60 and 240 min of intravenous injection is shown in Fig. 6. The radioactivity (counts per gram organ) in different organs 30 min post injection were found to be as follows: blood (13%), liver (24%), spleen (15%), lungs

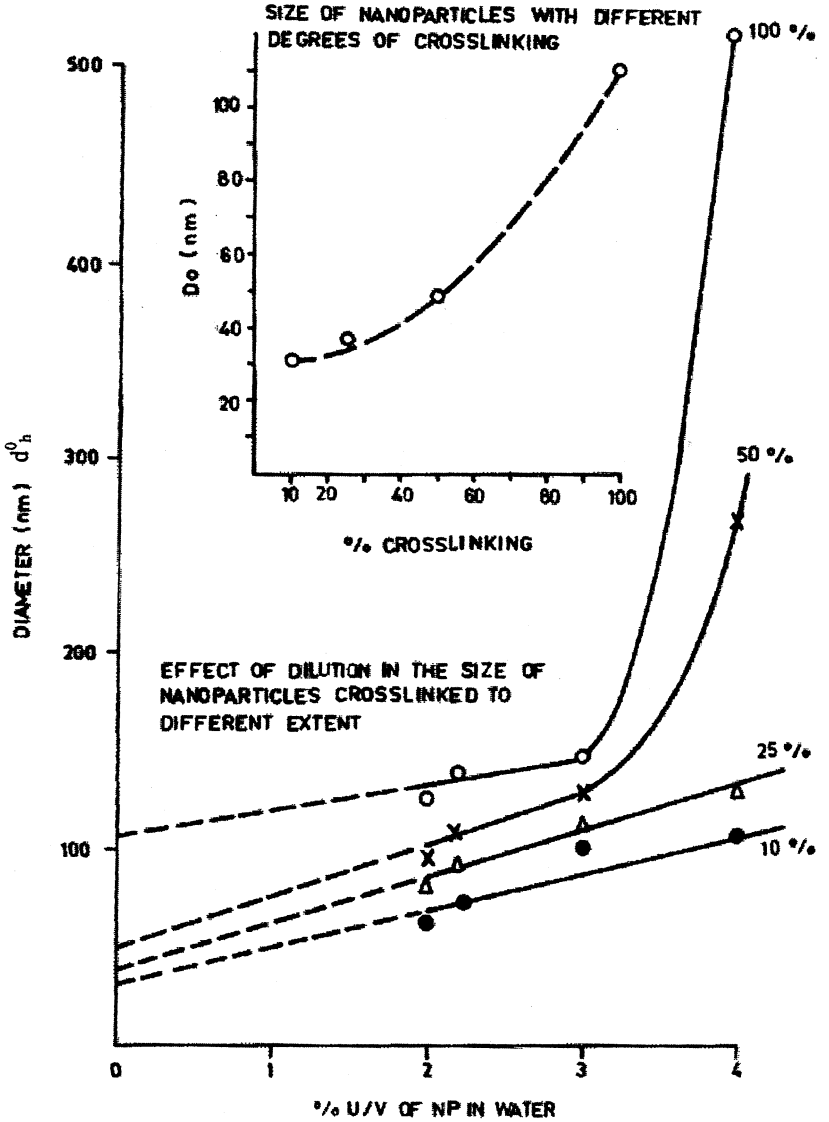

Fig. 3. Particle size variation in relation to particle density (% U/V) and percentage cross-linking (indicated at the right end of the figure). Inset: percentage cross-linking dependent particle size at infinite dilution.

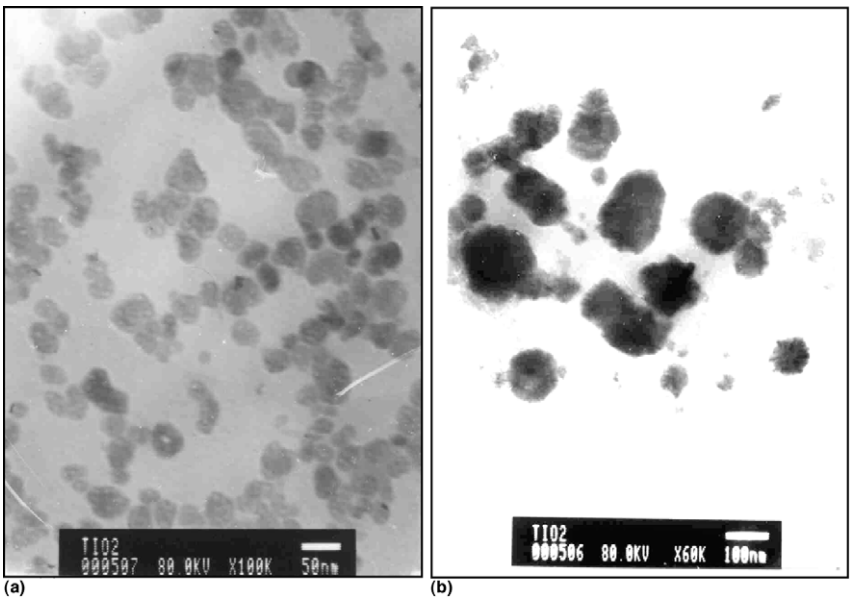

Fig. 4. Transmission electron micrographs of (a) 10% and (b) 100% cross-linked chitosan nanoparticles.

(9%), kidney and stomach (8%), while 5% activity was observed in bone and heart. The radioactivity recorded in the highly perfused organs, such as liver, spleen and lungs could be accounted for as the combined activity of the circulating blood passing through organs as well as that due to particle uptake by cells of the reticoendothelial system (RES) of these organs. Interestingly, after 1 h of administration, the radioactivity decreases substantially in the RES organs, but that in the blood circulation remains more or less constant indicating that RES uptake of these particles is not very significant. After 4 h of administration of nanoparticles, a considerable increase of radioactivity was observed in the stomach due to the accumulation of free ^{99m}Tc ions from the dissociation of the ^{99m}Tc–nanoparticle complex. The observation has been corroborated by analyzing the γ images of rabbit as shown in Fig. 7(a–c). After injecting radiolabeled chitosan nanoparticles (30 min), the γ image demonstrates intense radioactivity in the head and thoracic regions, in the liver, kidneys, vertebral column and the bladder (Fig. 7a, b). The entire blood pool can also be clearly observed in the image. Post injection (2 h) the liver, kidneys, vertebral column and bladder can be seen in the image (Fig. 7c). Therefore, the combined results of the biodistribution of ^{99m}Tc tagged chitosan nanoparticles in mice and γ images of rabbit clearly indicate long circulation of labeled nanoparticles in blood. Post injection (2 h), a clear observation of the blood pool in the γ image (Fig. 7c) corroborates this fact.

As previously reported by other workers the particle size, polymer composition and surface characteristic of nanoparticles determine the particle distribution profile and stability in the body (Van Oss, 1978; Tabata and Ikada, 1989; Vroman, 1991; Gref et al., 1994; Storm et al., 1995). Longer circulation of nanoparticles, with minimum uptake by the cells of RES is desirable in terms of better targetability of the nanoparticles. The major obstacle to active targeting of colloidal particles in the body system, has been the ability of the cells of the RES to rapidly remove intravenously applied particulates from the systemic circulation (Tomlinson and Davis, 1986). The usual strategy taken to avoid the uptake of nanoparticles is by coating the particle surface with hydrophilic polymers, like polyethylene glycol (PEG) derivatives such as poloxamers and poloxamines. It has been postulated by several

authors that decrease in uptake of PEG coated particles is possibly due to the presence of steric-barrier which decreases the adsorption of plasma proteins (opsonins) on the surface of these nanoparticles (Allen and Hansen, 1991). It has been demonstrated that the RES evasion and long

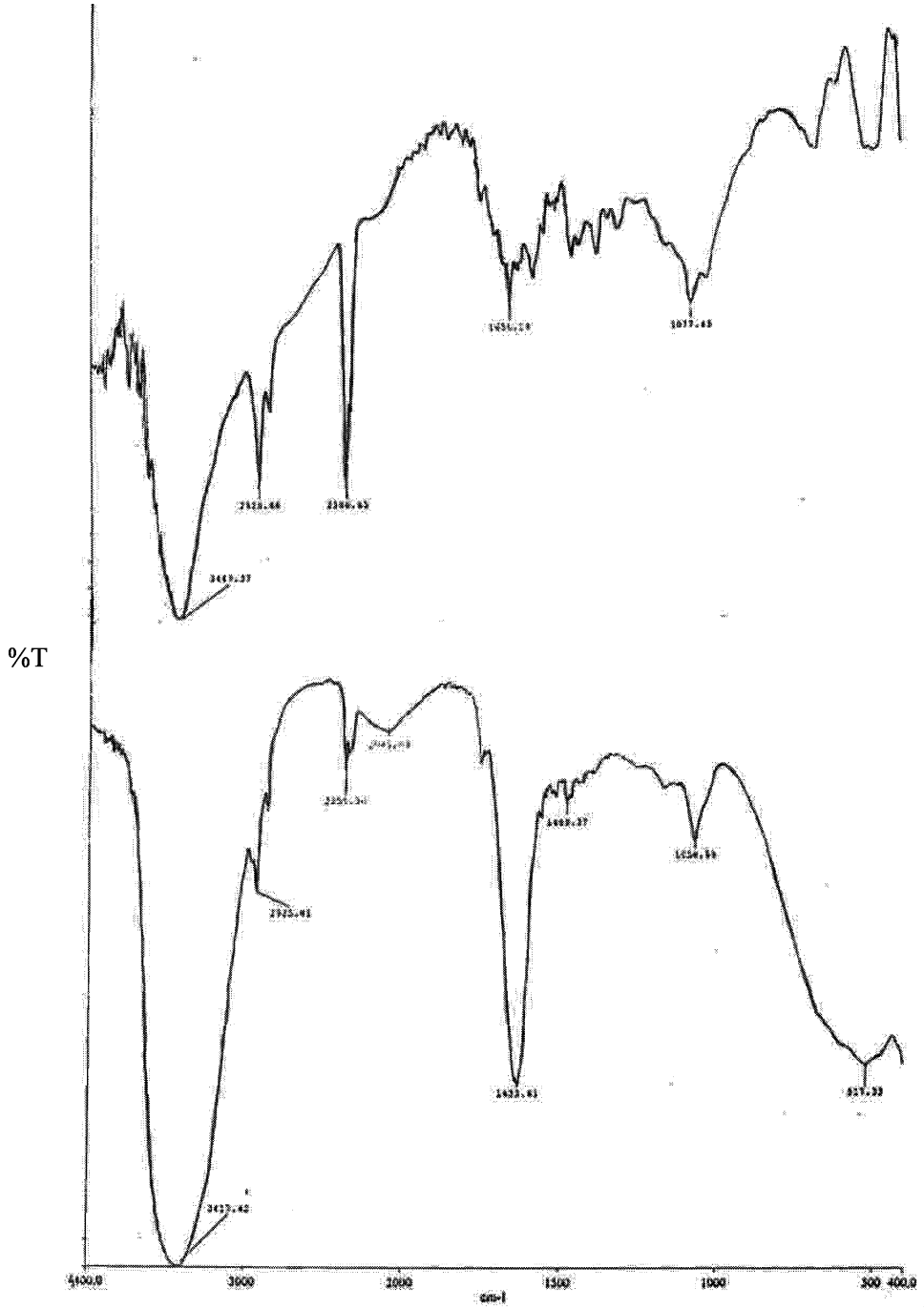

Fig. 5. FTIR spectra of (a) chitosan polymer and (b) cross-linked chitosan nanoparticles.

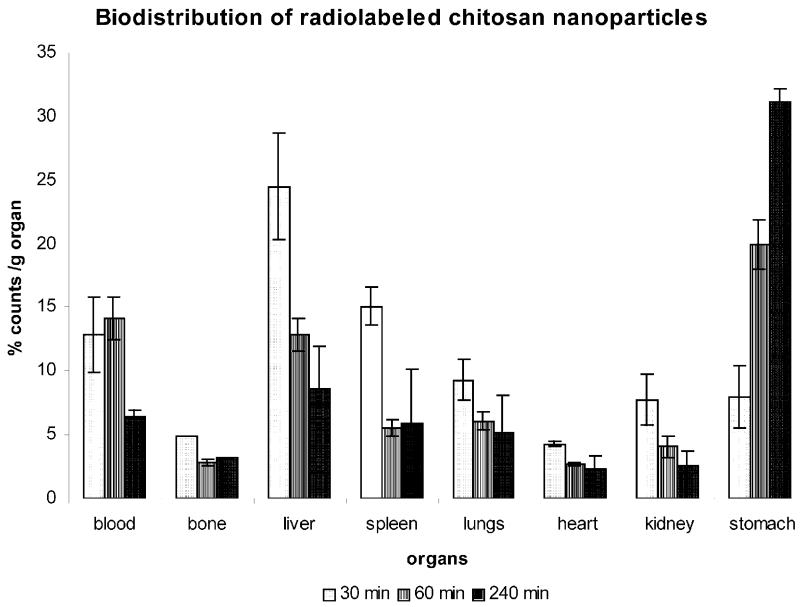

Fig. 6. Organ distribution of ^{99m}Tc radiolabeled chitosan nanoparticles, 30, 60 and 240 min post injection.

circulation by the particles are possible if the nanoparticles are of ultra-low size (usually < 100 nm diameter) and have surface hydrophilicity. By preparing nanoparticles of hydrogel polymers in the aqueous core of reverse micellar droplets, we have achieved both the characteristics of the particles and have demonstrated that these particles are RES evading and have long circulation in blood (Gaur et al., 2000). Chitosan being a hydrogel polymer forms nanoparticles with adequate surface hydrophilicity and hence these particles exhibits long circulation in blood even without surface PEGylation. Because of the limited stability of chitosan–^{99m}Tc complex we could not observe any significant radioactivity or any γ image beyond 4 h of injection.

In addition to the long circulating property of the nanoparticles, a small percentage of these nanoparticles are observed to be localized in the bone of the animals (Fig. 7a–c), 30 min and 2 h post injection with radiolabeled chitosan nanoparticles as well as in the biodistribution profile in mice (Fig. 6). The observation that the chitosan nanoparticles are accumulating in the bone albeit to a lesser extent (5%) in comparison to other body tissues, indicates that the polymer of the nanoparticles may be interacting with a blood component with high affinity for bone marrow endothelium. In a previous study by other workers, involving different co-polymer coated particles, the particles have been observed to be cleared by the sinusoidal endothelial cells of the bone marrow, where they become localized internally within the dense bodies of these cells (Porter et al., 1992). Considering that the chitosan nanoparticles are ultra-small (< 100 nm in diameter) and display the ability of localizing in the bone tissue, we can assume that they may have application in radio diagnostic imaging, other than use for drug delivery.

4. Conclusions

Ultra-low size (< 100 nm diameter) nanoparticles of water-soluble hydrogel polymer, such as chitosan, can be prepared in the aqueous core of reverse micellar droplets and can be cross-linked through glutaraldehyde. The size of the particles depends on the particle density as well as on the

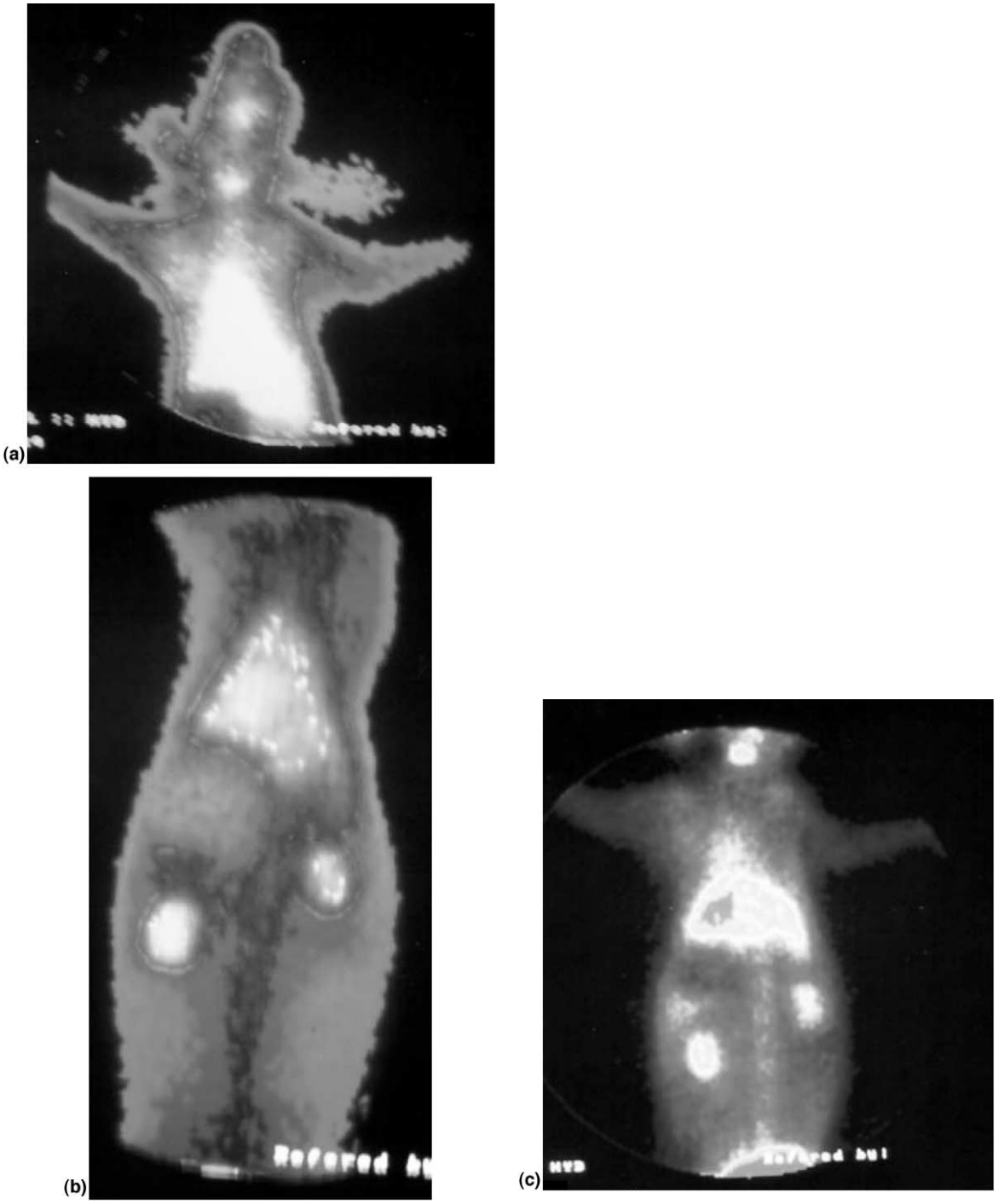

Fig. 7. Gamma images of rabbit, 30 min post injection (a, b) and 120 min post injection (c).

degree of cross-linking. For a particular degree of cross-linking, the particle size has been determined at infinite dilution of the particle solution. The particles have high level of radio labeling efficiency with ^{99m}Tc, although the complex is not very stable particularly beyond 4 h of preparation. The biodistribution and γ imaging of the chitosan nanoparticles establish that these particles are RES evading and circulate in the blood for considerable amount of time. Gamma imaging also confirms that a small amount of these particles goes to bone marrow also.

Acknowledgements

Dr T. Lazar Mathew, ex-Director, INMAS and Gen. T. Ravindranath, Director, INMAS are gratefully acknowledged for extending help and for their continuous encouragement and assistance throughout this study.

References

Aiedeh, K., Gianasi, E., Orienti, I., Zecchi, V., 1997. Chitosan microcapsules as controlled release systems for insulin. J. Microencapsul. 14, 567–576.

Akbuga, J., 1993. The effect of physicochemical properties of a drug on its release from chitosan malate tablets. Int. J. Pharm. 100, 257–261.

Allen, T.M., Hansen, C., 1991. Pharmacokinetics of stealth versus conventional liposomes: Effect of dose. Biochim. Biophys. Acta 1068, 133–141.

Allemann, E., Gurny, R., Deolker, E., 1993. Drug loaded nanoparticles: preparation methods and drug targeting issues. Eur. J. Pharm. Biopharm. 39, 173–191.

Alonso, M.J., Salve, P., Remunan-Lopez, C., Vilajato, J.L., 1998. Application of nanoparticles based on hydrophilic polymers as pharmaceutical forms. European Patent 0860-166-A1.

Bernkop-Schnurch, A., Krajicek, M.E., 1998. Mucoadhesive polymers as platforms for peroral peptide delivery and absorption: synthesis and evaluation of different chitosan-EDTA conjugates. J. Control. Rel. 50, 215–223.

Berscht, P.C., Nies, B., Liebendorfer, A., Kreuter, J., 1994. Incorporation of basic fibroblast growth factor into methylpyrrolidone chitosan fleeces and determination of the in vitro release characteristics. Biomaterials 15, 593–600.

Calvo, P., Remunan-Lopez, C., Vila-Jato, J.L., Alonso, M.J., 1997. Novel hydrophilic chitosan-poly (ethylene oxide) nanoparticles as protein carriers. J. Appl. Polym. Sci. 63, 125–132.

Douglas, S.J., Davis, S.S., Illum, L., 1986. Biodistribution of poly (butyl 2 cyanoacrylate) nanoparticles in rabbits. Int. J. Pharm. 34, 145–152.

Felt, O., Buri, P., Gurmy, R., 1998. Chitosan: a unique polysaccharide for drug delivery. Drug Dev. Ind. Pharm. 24, 979–993.

Gaur, U., Sahoo, S.K., De, T.K., Maitra, A.N., Ghosh, P.C., Ghosh, P.K., 2000. Biodistribution of fluoresceinated dextran using novel nanoparticles evading reticuloendothelial system. Int. J. Pharm. 202, 1–10.

Gref, R., Minamitake, Y., Peracchia, M.T., Trubetskoy, V., Torchilin, V., Langer, R., 1994. Biodegradable long circulating polymeric nanospheres, Science 263, 1600–1603.

Hou, M.J., Kim, M., Shah, D.O., 1988. A light scattering study on the droplet size and interdroplet interaction in microemulsion of AOT–oil water systems. J. Colloid Interface Sci. 123, 398–412.

Illum, L., 1998. Chitosan and its use as a pharmaceutical excipient. Pharm. Res. 15, 1326–1331.

Kawashima, Y., Lin, S.Y., Kasai, A., Handa, T., Takenaka, H., 1985. Preparation of a prolonged release tablet of aspirin with chitosan. Chem. Pharm. Bull. 33, 2107–2113.

Kristl, J., Smid-Korbar, J., Strue, E., Schara, M., Rupprecht, H., 1993. Hydrocolloids and gels of chitosan as drug carriers. Int. J. Pharm. 99, 13–19.

Leong, Y.S., Candau, F., 1982. Inverse microemulsion polymerization. J. Phys. Chem. 86, 2269–2271.

MacLaughlin, F.C., Mumper, R.J., Wang, J., Tagliaferri, J.M., Gill, I., Hinchcliffe, M., Rolland, A.P., 1998. Chitosan and depolymerized chitosan oligomers as condensing carriers for in vivo plasmid delivery. J. Control. Rel. 56, 259–272.

Maitra, A.N., 1984. Determination of size parameters of water–Aerosol OT–oil reverse micelles from their nuclear magnetic resonance data. J. Phys. Chem. 88, 5122.

Maitra, A.N., Ghosh, P.K., De, T.K., Sahoo, S.K., 1999. Process for the preparation of highly monodispersed hydrophilic polymeric nanoparticles of size less than 100 nm. US Patent 5,874,111.

Mitra, S., De, T.K., Maitra, A.N., 2002. Hydrogel nanoparticles: their applications in drug delivery. Encyclopedia of Surface and Colloid Science 2397–2413.

Munshi, N., Chakravarty, K., De, T.K., Maitra, A.N., 1995. Activity and stability studies of ultrafine nanoencapsulated catalase and penicillinase. J. Colloid Polym. Sci. 273, 464.

Munshi, N., De, T.K., Maitra, A.N., 1997. Size modulation of polymeric nanoparticles under controlled dynamics of microemulsion droplets. J. Colloid Interface Sci. 190, 000–000.

Nigalaye, A.G., Adusumilli, P., Bolton, S., 1990. Investigation of prolonged drug release from matrix formulations of chitosan. Drug Dev. Ind. Pharm. 16, 449–467.

Nishioka, Y., Kyotani, S., Okamura, M., Miyazaki, M., Okazaki, K., Ohnishi, S., Yamamoto, Y., Ito, K., 1990. Release characteristics of cisplatin chitosan microspheres

and effect of containing chitin. Chem. Pharm. Bull. 38, 2871–2873.

Porter, C.J.H., Moghimi, S.M., Illum, L., Davis, S.S., 1992. The polyoxymethylene/polyoxypropylene block co-polymer poloxomer 407 selectively redirects intravenously injected microspheres to sinusoidal endothelial cells of rabbit bone marrow. FEBS Lett. 305, 62–67.

Robert, C., Bwu, P., Pappas, N.A., 1988. Experimental methods for bioadhesive testing of various polymers. Acta Pharm. Technol. 34, 95–98.

Roy, K., Mao, H.Q., Huang, S.K., Leong, K.W., 1999. Oral gene delivery with chitosan–DNA nanoparticles generates immunologic protection in a murine model of peanut allergy. Nat. Med. 5, 387–391.

Storm, G., Belliot, S.O., Daemen, T., Lasic, D.D., 1995. Surface modification of nanoparticles to oppose uptake by mononuclear phagocyte system. Adv. Drug Del. Rev. 17, 31–48.

Tabata, Y., Ikada, Y., 1989. Protein precoating of polylactide microspheres containing a lipophilic immunopotentiator for enhancement of macrophage phagocytosis and activation. Pharm. Res. 6, 296–301.

Thanoo, B.C., Sunny, M.C., Jayakrishnan, A., 1992. Cross-linked chitosan microspheres: preparation and evaluation as a matrix for the controlled release of pharmaceuticals. J. Pharm. Pharmacol. 44, 283–286.

Theobald, A.E., 1990. In: Sampson, C.B. (Ed.), Textbook of Radiopharmacy: Theory and Practice. Gorden and Breach, NY, p. 127 Chapter 7.

Tomlinson, E., Davis, S.S. (Eds.), 1986. Site-Specific Drug Delivery: Cell Biology, Medicinal and Pharmaceutical Aspects. Wiley, Chichester.

Tozaki, H., Komoike, J., Tada, C., Maruyama, T., Terabe, A., Suzuki, T., Yamamoto, A., Muranishi, S., 1997. Chitosan capsules for colon-specific drug delivery: improvement of insulin absorption from the rat colon. J. Pharm. Sci. 86, 1016–1021.

Van Oss, C.J., 1978. Phagocytosis as a surface phenomenon. Annu. Rev. Microbiol. 32, 19–39.

Vroman, L., 1991. Proteins in blood plasma at interfaces. In: Bender, M. (Ed.), Interfacial Phenomena in Biological Systems, Surfactant Science Series. Marcel Dekker, New York, pp. 136–150.